

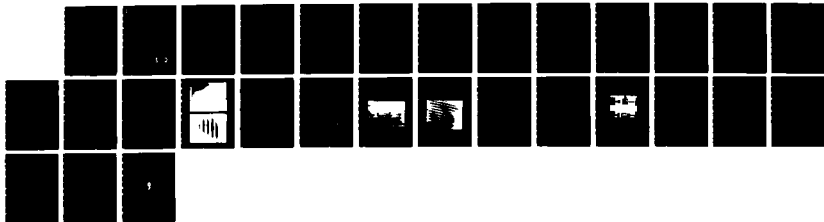
AD-A177 518

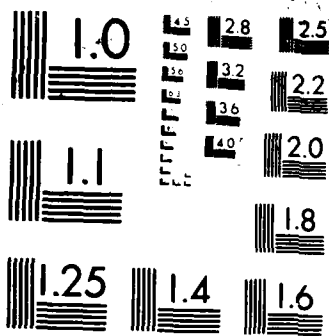
RESEARCH ON MATERIALS AND COMPONENTS FOR  
OPTO-ELECTRONIC SIGNAL PROCESSING AND COMPUTING(U)  
CALIFORNIA UNIV SAN DIEGO LA JOLLA W S CHANG ET AL  
30 DEC 86 AFOSR-TR-87-0268 AFOSR-84-0389 F/G 17/8

1/1

UNCLASSIFIED

ML





MICROCOPY RESOLUTION TEST CHART  
NATIONAL BUREAU OF STANDARDS-1963-A

SECURITY CLASSIFICATION

## REPORT DOCUMENTATION PAGE

1a. REPORT SECURITY CLASSIFICATION Unclassified		1b. RESTRICTIVE MARKINGS	
2a. SECURITY CLASSIFICATION AUTHORITY		3. DISTRIBUTION/AVAILABILITY OF REPORT Approved for public release; distribution unlimited.	
2b. DECLASSIFICATION/DOWNGRADING SCHEDULE		4. PERFORMING ORGANIZATION REPORT NUMBER(S)	
5. MONITORING ORGANIZATION REPORT NUMBER(S) AFOSR-TR 87-0268		6a. NAME OF PERFORMING ORGANIZATION The Regents of the University of California	
6b. OFFICE SYMBOL (If applicable)		7a. NAME OF MONITORING ORGANIZATION Dr. C. Lee Giles AFOSR/NE	
6c. ADDRESS (City, State and ZIP Code) University of California, San Diego La Jolla, CA 92093		7b. ADDRESS (City, State and ZIP Code) Bolling Air Force Base Washington, D.C. 20332	
8a. NAME OF FUNDING/SPONSORING ORGANIZATION Dept. of the Air Force		9. PROCUREMENT INSTRUMENT IDENTIFICATION NUMBER AFOSR 84-0389	
8b. OFFICE SYMBOL (If applicable) NE		10. SOURCE OF FUNDING NOS.	
8c. ADDRESS (City, State and ZIP Code) AFOSR/PKD Building 410 Bolling AFB, D.C. 20332-6448		PROGRAM ELEMENT NO. 61102F FQ8671	PROJECT NO. 2305 8600358
11. TITLE (Include Security Classification) Research on Materials and Components for Opto-Electronic Signal Processing & Computing		TASK NO. B1 2305/B1	WORK UNIT NO.
12. PERSONAL AUTHOR(S) William S.C. Chang, Albert L. Kellner, C.C. Sun, Timothy Van Eck and H.H. Wieder			
13a. TYPE OF REPORT Interim Report		13b. TIME COVERED FROM 12/1/85 TO 11/30/86	
14. DATE OF REPORT (Yr., Mo., Day) 1986, December 30		15. PAGE COUNT	
16. SUPPLEMENTARY NOTATION			
17. COSATI CODES		18. SUBJECT TERMS (Continue on reverse if necessary and identify by block number)	
FIELD	GROUP	SUB GR	III-V Compound Semiconductors, Electro-absorption, Electro-refraction, Gate Controlled Photodiode, Quantum Wells
19. ABSTRACT (Continue on reverse if necessary and identify by block number) Electro-absorption and electro-refraction properties of heterostructures and multiple quantum-well structures in III-V semiconductors were investigated for spatial modulation applications. A new device, the gate controlled photo-diode (GCPD) has been conceived and demonstrated. It has potential applications in optical signal processing.			
<div style="display: flex; justify-content: space-around; align-items: center;"> <div style="text-align: left;"> <p style="font-size: 2em; font-weight: bold;">DTIC FILE COPY</p> </div> <div style="text-align: center;"> <p style="font-size: 3em; font-weight: bold; letter-spacing: 0.5em;">S DTIC ELECTE D</p> <p style="font-size: 1.5em; font-weight: bold;">MAR 02 1987</p> <p style="font-size: 2em; font-weight: bold;">D</p> </div> </div>			
20. DISTRIBUTION/AVAILABILITY OF ABSTRACT UNCLASSIFIED/UNLIMITED <input checked="" type="checkbox"/> SAME AS RPT. <input type="checkbox"/> DTIC USERS <input type="checkbox"/>		21. ABSTRACT SECURITY CLASSIFICATION Unclassified	
22a. NAME OF RESPONSIBLE INDIVIDUAL Dr. C. Lee Giles		22b. TELEPHONE NUMBER (Include Area Code) (202) 767-4931	
22c. OFFICE SYMBOL NE		22d. OFFICE SYMBOL	

INTERIM ANNUAL TECHNICAL REPORT  
RESEARCH ON MATERIALS AND COMPONENTS FOR  
OPTO-ELECTRONIC SIGNAL PROCESSING AND COMPUTING

~~AFOSR-TB~~ 87-0268

**1. Introduction and Overview**

It has been recognized for some time that optical signal processing and optical computing hold considerable promise for high-speed signal processing in DoD applications due to their parallel processing capabilities. In III-V compound semiconductors, optical devices, such as lasers and detectors, have already been realized. Electronic devices such as GaAs MESFET, the InP MISFET and the HEMT have also been demonstrated. Electronic and optical devices could potentially be integrated monolithically on the same chip. However, there are many unresolved issues such as how to obtain efficient modulation and how to integrate different devices on the same chip. Substantially more research in materials and components (including microfabrication processing technology) must be undertaken before the full potential of combined opto-electronic signal processing and computing using III-V compound semiconductors can be realized.

For optical computing, spatial light modulators that operate at very high speed and that require very low switching energy are urgently needed. The conventional electro-optical coefficients of III-V compound semiconductors are too small to be useful for efficient spatial modulation. Multiple quantum well structures hold great promise for spatial light modulation because they exhibit a strong and sharp excitonic absorption line. The wavelength of the absorption peak can be tuned by and is very sensitive to the applied electric field. Thus, for radiation wavelength slightly longer than the wavelength of the exciton absorption line, the transmission of this radiation through the quantum well materials would be modulated efficiently by applying an electric field. Spatial light modulators utilizing such



controlled photo diode will be brought to a conclusion by June, 1987. The investigation of the nonlinear effects in  $\text{In}_{0.53}\text{Ga}_{0.47}\text{As}/\text{Al}_{0.48}\text{In}_{0.52}\text{As}$  will be shifted to some other programs.

## 2. Electro-Optic Modulation in InGaAs/GaAs Multiple Quantum Well

### Structures

Multiple quantum well structures have great promise for spatial light modulation because they exhibit a strong, sharp, excitonic absorption peak which is very sensitive to an applied electric field.<sup>(1)</sup> The InGaAs/GaAs material system was chosen for this work because of the optical wavelength at which it has useful electro-absorption properties. In the commonly used GaAs/AlGaAs material system, the GaAs substrate is opaque at the wavelength of interest, but it is transparent at the operating wavelength of the  $\text{In}_x\text{Ga}_{1-x}\text{As}/\text{GaAs}$  system. Thus,  $\text{In}_x\text{Ga}_{1-x}\text{As}/\text{GaAs}$  multiple quantum well structures can be used for spatial light modulation without removing the substrate from the structure.  $\text{In}_x\text{Ga}_{1-x}\text{As}$  has other advantages over AlGaAs; it is easier to grow by MBE because its growth temperature is lower, and there is no evidence of deep level traps in InGaAs, such as those found in AlGaAs. Finally, the  $\text{In}_x\text{Ga}_{1-x}\text{As}/\text{GaAs}$  material system is emerging as an important material system for other electronic and opto-electronic devices such as high electron mobility transistors<sup>(2)</sup> and avalanche photo diodes,<sup>(3)</sup> so the development of this material system is likely to continue at an accelerated pace.

Because  $\text{In}_x\text{Ga}_{1-x}\text{As}$  and GaAs are not lattice-matched, this material system has some potential fabrication problems. If a thick  $\text{In}_x\text{Ga}_{1-x}\text{As}$  epitaxial layer is grown on a GaAs substrate, the lattice mismatch between the materials will be accommodated by misfit dislocations in the  $\text{In}_x\text{Ga}_{1-x}\text{As}$ . These misfit dislocations would make the material non-uniform. A non-uniform quantum well would have a very broad exciton absorption line and would thus be useless for electro-optic modulation. However, if the  $\text{In}_x\text{Ga}_{1-x}\text{As}$  layer thickness is kept below a certain critical thickness, the lattice mismatch will be accommodated by strain in the  $\text{In}_x\text{Ga}_{1-x}\text{As}$  rather than by misfit dislocations.<sup>(4)</sup> In this case, the epitaxial layer is

said to be pseudomorphic. The question of whether many alternating layers of two non-lattice-matched materials will be pseudomorphic is only slightly more complex. Each individual layer must be thinner than the critical thickness. For the purpose of calculating the critical thickness of a multiple quantum well structure, the region containing alternating layers may be considered as a single layer, with a composition equal to the average of two compositions weighted by their thicknesses, and a thickness equal to the total thickness of the region.<sup>(5)</sup> For a pseudomorphic epitaxial layer, the lattice of the substrate is perfectly preserved in the epitaxial layer; consequently, the  $\text{In}_x\text{Ga}_{1-x}\text{As}$  is strained. This strain alters the conduction and valence band energies, so that the bandgap of  $\text{In}_x\text{Ga}_{1-x}\text{As}$  is a function of its strain.<sup>(6)</sup> In addition, the heavy-hole and-light hole valence bands, which are normally degenerate in energy, are split in energy by the strain. As a result, we expect the heavy-hole and light-hole exciton peaks to be isolated from each other (unlike in GaAs/AlGaAs quantum wells, where they are very close in energy). The isolation of the exciton peaks should allow us to better understand the physics of quantum well electro-absorption, since we can observe the effects of an electric field on a non-degenerate exciton absorption peak.

The first step in our work with this material system was to grow high-quality  $\text{In}_x\text{Ga}_{1-x}\text{As}$  and GaAs by molecular beam epitaxy (MBE) under identical growth conditions, and to determine the composition and growth rate of the InGaAs that was grown so that the desired composition and layer thickness could be obtained in subsequent growths. Following that, a multiple quantum well (MQW) structure, designated MBE-110, was grown by MBE. This structure consists of alternating layers of 100 Å thick  $\text{In}_{0.12}\text{Ga}_{0.88}\text{As}$  quantum wells and 150 Å thick GaAs barriers, ten layers each. Nomarski optical microscopy of a non-pseudomorphic epitaxial layer usually reveals a characteristic cross-hatched pattern; the lack of such a pattern on the surface of MBE-110 indicates that it is pseudomorphic. This is confirmed by lattice-imaging cross-sectional transmission electron microscope photographs made at Lockheed Research Laboratories and reproduced here as Figure 1. The quantum well and barrier layers were undoped and were sandwiched between n-type and p-type

layers, on which ohmic contacts were fabricated. Thus, the quantum wells were in the intrinsic region of a p-i-n diode, and a nearly uniform electric field perpendicular to the quantum wells was applied by applying a reverse voltage to the diode. A schematic diagram of the sample is shown in Figure 2.

The room-temperature absorption spectrum of the MQW sample was measured by measuring the sample's transmittance as a function of wavelength. The effects of surface reflection and residual substrate absorption were cancelled out by simultaneously measuring the transmittance of the MQW sample and a plain GaAs wafer polished to the same thickness. The electro-absorption spectra were measured by synchronizing the laser pulse with a short-duration reverse voltage pulse applied to the sample. The results of the electro-absorption measurements are shown in Figure 3. Only one absorption peak is observed instead of the two peaks seen in GaAs/AlGaAs quantum wells because of the large strain-splitting of the heavy-hole and the light-hole valence bands. When a voltage is applied to the sample, the absorption peak shifts slightly to lower energy and weakens dramatically. With only 2 V applied to the device, 6.4% intensity modulation is obtained at a wavelength of .94  $\mu\text{m}$ . This rate of modulation per quantum well is comparable to that reported for GaAs/AlGaAs quantum wells.<sup>(1)</sup> These results have been reported in *Applied Physics Letters*<sup>(7)</sup> and at the Annual Meeting of the Optical Society of America.<sup>(8)</sup>

While these results demonstrate that strong electro-absorption can be obtained in pseudomorphic  $\text{In}_x\text{Ga}_{1-x}\text{As}/\text{GaAs}$  quantum wells, further research is needed in three areas:

- (1.) To use the epitaxially grown material most efficiently, we are studying how to maximize the electro-absorption per quantum well by changing the parameters of the quantum well, such as its thickness.
- (2.) In order to obtain a useful amount of optical modulation, such as 50%, a much larger number of quantum wells, such as 100, will be needed. The cumulative effect of the strain may limit the maximum number of layers that may be grown pseudomorphically. The strain will also be larger for higher concentrations of In, i.e., x. Thus, in

addition to the limitation in the maximum number of pseudomorphic layers, there may also be a limitation on the wavelength of the exciton absorption that may be tuned by changing the  $x$ . For example, in order to obtain modulation of the  $1.06 \mu\text{m}$  radiation of the Nd/YAG laser,  $x$  needs to be of the order of 0.25. The crystalline quality of the  $\text{In}_x\text{Ga}_{1-x}\text{As}$  layer may also affect the sharpness of the exciton absorption. However, for electro-absorption, it may not be necessary for the quantum wells to be grown pseudomorphically to the substrate; only uniformity of the crystal lattice is required. The quantum wells could be grown pseudomorphically on a buffer layer with a lattice constant different than the substrate.<sup>(9)</sup> A set of structures designed to test both the effect of the strain and the technique of using a buffer layer has been fabricated. Two structures are grown directly on a GaAs substrate, consisting nominally of  $100 \text{ \AA}$   $\text{In}_{0.25}\text{Ga}_{0.75}\text{As}$  quantum wells and  $200 \text{ \AA}$  GaAs barriers. Both have ten quantum wells; MBE-236 has a GaAs cap and MBE-237 does not. Cross-sectional transmission electron microscope photographs show a very high density of dislocations in these structures, as shown in Figure 4. A third structure, MBE-238, is identical to MBE-237 except that it is grown on a thick layer of  $\text{In}_{0.08}\text{Ga}_{0.92}\text{As}$ . It is believed that the lattice constant of the thick  $\text{In}_{0.08}\text{Ga}_{0.92}\text{As}$  buffer is relaxed to its bulk lattice constant, and is therefore equal to the average lattice constant of the multiple quantum well material. The critical thickness is then effectively infinite, and the entire multiple quantum well region, no matter how thick it is, should be pseudomorphic to the buffer layer. Transmission electron microscope photographs of MBE-238 (Fig. 5) do not show dislocations like the ones seen in MBE-236 and MBE-237. Future research will involve the growth of a large number of quantum wells, and an investigation of whether such quantum wells are as effective for electro-absorption as pseudomorphic quantum wells grown on GaAs.

- (3.) The ultimate objective of this project is an optically-addressed spatial light modulator. A pixel for such a device would require initially an electro-absorption modulator and a photo-detector fabricated on the same substrate. If such a spatial light modulator is to have high sensitivity, it must also have gain in each pixel, so each pixel must eventually have either a detector with gain, such as a photo-transistor or avalanche photo-diode, or a transistor must be fabricated together with the modulator and photo-detector. A simple initial hypothetical structure for a single pixel of a future spatial light modulator array may appear like the device sketched in Figure 6. In this case, the controlling radiation will be incident on the SLM from the top side, while the signal radiation to be modulated will be incident from the bottom side. The controlling and the signal radiations are at the same wavelength. The detector p-n diode structure may be grown epitaxially first, followed by the etching of the modulator area and the regrowth of the MQW p-n structure for the modulator. Etch and regrowth of MQW layers have not been done before. However, we do not expect any fundamental difficulties in the regrowth process since there is no Al that may oxidize before the regrowth. Both the p-n detector diode and the p-n MQW modulator diode are connected in parallel by the metallization pattern to the power supply through a load resistor. The MQW modulator will not sense the controlling radiation because of the metal reflector. The composition of the  $\text{In}_y\text{Ga}_{1-y}\text{As}/\text{GaAs}$  in the detector will be designed to absorb the controlling radiation under a wide range of bias voltage. The photo-current generated by the controlling radiation through the detector will change the reverse bias voltage applied to the MQW produced by the voltage drop across the load resistor. Changes in the electro-absorption of the MQW produced by the change in bias voltage will then modulate the reflected signal radiation. The metal layer enhances the reflection. The detector is shielded from the signal radiation by the heavily doped (non-depleted)  $\text{In}_z\text{Ga}_{1-z}\text{As}/\text{GaAs}$  absorber layer. Such a modulator/detector pair is similar to the SEED device reported in the literature.<sup>(10)</sup> The primary difference is that

the detector diode is separated from the modulator diode in our device so that the controlling radiation and the signal radiation are isolated from each other. Such a structure is more suitable for optical computing applications.

Clearly, an important device in the unit cell is the photo-detector that should have high speed, low leakage current, low noise and high sensitivity, and that is compatible with the materials and fabrication processes required for the modulator. Electrically, both the detector and the modulator can be represented by two capacitors in parallel with a total capacitance  $C$ . The photo-current  $i_{ph}$  from the detector creates a reduction of the bias voltage  $V$  across both the detector and the modulator through the voltage drop of the load resistor ( $i_{ph}R_L$ ) with the time constant  $R_L C$ . The larger  $i_{ph}$ , the smaller the  $R_L$  required to create the necessary voltage drop, and the faster the switching time constant  $R_L C$ . However, a large  $i_{ph}$  requires a large optical intensity. Our estimation shows that the photo-current generated by the detector without amplification is not enough to achieve switching with low optical intensity at very high speed. Thus, the speed of a SEED device will be limited by this factor. Our proposed structure differs fundamentally from a SEED device in that the amplification of the detector current may be accomplished in a future version of the device. For example, the p-i-n detector shown in Figure 6 may be replaced in the future by an avalanche diode, a p-n-diode-FET combination or photo transistor to provide gain. The situation is complicated further by the photo-current generated in the electro-absorption process of the signal radiation itself (i.e., some kind of self-absorption or bleaching). The fabrication and characterization of the detector-modulator pair will be a major effort in 1987, followed by a demonstration of 2 x 2 spatial modulator. Research on the amplification of the detector current will follow immediately after that demonstration, probably not in 1987.

Associated with the excitonic electro-absorption spectrum is an electro-refraction effect that occurs within the same range of wavelengths. For some applications, phase modulation

is more useful than intensity modulation. Electro-refraction could also be used to obtain intensity modulation when the sample is coated with dielectric reflecting coatings to obtain Fabry-Perot resonance. Such an intensity modulator does not depend on absorption. Thus, electro-refraction may reduce substantially the photo-current that may be generated by the signal radiation. An investigation of electro-refraction in quantum wells has been undertaken. The MQW structures fabricated thus far at UCSD do not have enough quantum wells for an accurate measurement of electro-refraction, so a 60-quantum well sample was obtained from MIT Lincoln Laboratory.<sup>(11)</sup> This InGaAs/GaAs sample has quantum wells very similar to those described above, and has electro-absorption spectra similar to those described above, but much stronger because it has six times as many quantum wells. Electro-refraction was measured interferometrically as it was previously in bulk materials.<sup>(12)</sup> The results are shown in Figure 7. The solid curve in Figure 7b represents a numerical calculation of the electro-refraction based on the Kramers-Kronig transform of the measured electro-absorption data shown in Figure 7a: the main features of the electro-absorption and electro-refraction are consistent with each other. Notice that the change of index that can be obtained by electro-refraction is much larger than that which can be obtained in  $\text{LiNbO}_3$ . However, this experiment also demonstrates that, despite a large change of refractive index (up to .03) which can be induced by electro-refraction, the corresponding phase change, 15 mrad, is fairly small because of the small path length. For a phase modulation of  $\pi$  radians, it appears that either a large number of quantum wells (e.g., 1000) is required or a device with multiple paths must be employed. Furthermore, at wavelengths where the electro-refraction is large, there will always be some absorption and electro-absorption. Further research is required to characterize the electro-refraction effect. For spatial light intensity modulation, a Fabry-Perot etalon based on the electro-refractive medium needs to be investigated. For spatial phase modulation, research needs to be undertaken on (1) the minimum phase shift that may be required for specific applications, (2) device structures that may be less sensitive to absorption, and (3) materials growth technology for producing samples with

very large numbers of quantum wells.

### 3. The Gate Controlled Photo Diode and Applications

During the previous grant period, we have conceived and demonstrated a new device, the gate controlled photodiode (GCPD). The multiplication of the gate voltage  $V_g$  and the optical radiation intensity  $P_L$  has already been demonstrated with 3% nonlinearity of the photo-current output within a dynamic range of 30 dB for both  $V_g$  and  $P_L$ . However, the response time was limited to 100 nsec with the 15  $\mu\text{m}$  long gate device. During the current grant period, a GCPD with stepped gate-oxide thickness, as shown in Fig. 8, has been conceived, fabricated and evaluated. In this device the poly-Si gate with total length  $L = 15 \mu\text{m}$  is divided into three 5- $\mu\text{m}$ -long sections. The oxide thicknesses of the three sections are 700 Å, 1500 Å and 3000 Å respectively. For this device, 10 nsec response time has been obtained. Fig. 9 shows the response time of all the devices fabricated. The dashed line represents the predicted response time based upon diffusion. The fast response of the stepped gate-oxide thickness device is attributed to the component of the electric field parallel to the oxide-Si interface created by the non-uniform electrical surface potential in Si. Such an electric field component would increase the drift velocity in that direction.

We had estimated earlier that in order for GCPD to be superior to other competitive devices, we need to achieve a linearity better than 3% within a 30 dB dynamic range of both  $V_g$  and  $P_L$  within a response time of 1 nsec. Thus, the understanding and the characterization of the response time is an important issue. In order to further understand the mechanisms and the relative importance of drift and diffusion, we are now fabricating GCPD with three isolated section of the gate so that they can be biased at different voltages.

GCPD's are naturally connected in a row in parallel for the photo-current in all these devices when a heavily doped collector bar is used for the common collector of all these devices as shown in Fig. 10. The gate electrodes of GCPD's in different columns can easily be connected in parallel for these devices in a column by means of the poly-Si electrode. Thus,

array of the GCPD shown in Fig. 11 would perform the matrix multiplication of  $\vec{A} \cdot \underline{X}$  where  $A_{ij}$  is the optical intensity in each pixel and  $X_j$  is the voltage applied to each column. The major advantage of using a GCPD array for matrix multiplication is that the interconnection architecture of all the pixels is extremely simple and effective. The delay of the signals propagating along the interconnections is very short.

For matrix computation in signal processing applications, we need to solve for  $\underline{X}$  where  $\vec{A}$  and  $\underline{Y}$  are  $\underline{Y} = \vec{A} \cdot \underline{X}$ . In the iterative method,<sup>(13)</sup> the solution of  $\underline{X}$  is obtained through an iterative procedure where an initial estimate of  $\underline{X}$  is used to calculate the next order of estimation through the relationship

$$\underline{X}_{i+1} = (\vec{I} - \vec{A}) \cdot \underline{X}_i + \underline{Y} = \vec{B} \cdot \underline{X}_i + \underline{Y}$$

Here  $\vec{I}$  is the identity matrix and  $i$  is the order of iteration. When the iterative procedure converges, then  $\underline{X}_{i+1} \cong \underline{X}_i$  and the  $\underline{X}_i$  in the above equation satisfies the relation,  $\underline{Y} = \vec{A} \cdot \underline{X}$ . Fig. 12 show the scheme in which GCPD's may be used for such a matrix manipulation procedure. Any analog method for solving  $\underline{X}$  is inferior to the digital method because of its accuracy limitation. However, in many applications for which real-time solution is needed, a low degree of accuracy is acceptable. For these applications, analog parallel processing would be the desirable method because of its speed. For example, the analog solution may be used as the initial estimation for an accurate digital process. Since the analog solution is already a close initial estimation, the digital calculation can be performed at a very high speed. Comparing the use of GCPD array with other methods for analog matrix computation, we see that the speed of the GCPD matrix computation will be limited only by the speed of response of GCPD which is already much faster than those schemes using presently-available spatial light modulators. There is very little propagation delay. The GCPD array is simple to fabricate, thus one can potentially obtain a large array (e.g. 1000  $\times$  1000 pixels). Such a large array would increase the overall speed of the matrix computation because of the increase of the number of parallel channels.

#### 4. Properties of InGaAs/AlInAs Quantum Wells on InP

In order to investigate the nonlinear properties of the  $\text{In}_{0.53}\text{Ga}_{0.47}\text{As}/\text{Al}_{0.48}\text{In}_{0.52}\text{As}$  quantum wells in optical waveguides, we have concentrated on the growth and the characterization of the InGaAs and AlInAs layers in InP substrates. Excellent layers of AlInAs and InGaAs have been grown by MBE on InP substrates. For example, in a research project sponsored by TRW, a GaAs/InGaAs High Electron Mobility Transistor (HEMT) device has been made. It has exhibited a transconductance of 190 ms/mm with a 1  $\mu\text{m}$  long gate. In a second project, an  $\text{In}_{0.43}\text{Al}_{0.57}\text{As}$  layer was grown in InP as an insulated gate field effect transistor with a mobility of 3000  $\text{cm}^2/\text{V}\cdot\text{sec}$ . Optically, the change of bandgap  $E_g$  as a function of the composition of  $\text{In}_x\text{Al}_{1-x}\text{As}$  has been measured by photoluminescence. This result is shown in Fig. 13. Good optical surface quality was obtained in all these layers. The variation of  $E_g$  means that the composition of Al can be used to control the optical index while maintaining the integrity of the crystalline structure. In a multilayer waveguide, it means that the waveguide index profile can be tailored to fit specific applications. Experiments to excite the guided wave mode in AlInAs waveguide are currently being conducted. However,  $\text{In}_{0.53}\text{Ga}_{0.47}\text{As}/\text{Al}_{0.48}\text{In}_{0.52}\text{As}$  multiple quantum well and single quantum well structures have only shown very broad photoluminescence spectra at 4° K. The cause for the absence of sharp exciton lines in these materials while exhibiting excellent electronic properties is currently being investigated under another research program.

#### 5. Papers Presented, Published and Submitted During the Contract Period

1. T.E. Van Eck, P. Chu, W.S.C. Chang and H.H. Wieder, "Electro-Absorption in an InGaAs/GaAs Strained Layer Multiple Quantum Well Structure", *Appl. Phys. Lett.*, **49**, 135-136 (1986).

2. T.E. Van Eck, L.M. Walpita, W.S.C. Chang and H.H. Wieder, "Franz-Keldysh Electro-Refraction and Electro-Absorption in Bulk InP and GaAs", *Appl. Phys. Lett.*, **48**, 451-453 (1986).
3. T.E. Van Eck, P. Chu, W.S.C. Chang and H.H. Wieder, "Electro-Optic Modulation in an InGaAs/GaAs Strained Layer Multiple Quantum Well Structure", Paper presented at the Optical Society of American Annual Meeting, Seattle, Washington (1986).
4. W.S.C. Chang, H.H. Wieder, T.E. Van Eck, A.L. Kellner and P. Chu, "Electro-Optical Properties of III-V Compound Semiconductors for Spatial Light Modulation Applications", SPIE Advanced Institute on Hybrid and Optical Computers, Leesburg, VA, March (1986).
5. T.E. Van Eck and W.S.C. Chang, "Electro-Refraction in an InGaAs/GaAs Multiple Quantum Well Structure". Paper submitted.
6. C.C. Sun, W.S.C. Chang and H.H. Wieder, "The Gate Controlled Photo-diode for Optical Matrix Multiplication Applications", Paper presented in the SPIE International Symposium on Optical and Opto-Electronic Engineering, San Diego, CA, August (1986).

## 6. References

1. T.H. Wood, C.A. Burrus, D.A.B. Miller, D.S. Chemla, T.C. Damen, A.C. Gossard, and W. Wiegmann, *Appl. Phys. Lett.*, **44**, 16 (1984).
2. J.J. Rosenberg, M. Benlamri, P.D. Kirchner, J.M. Woodall and G.D. Pettit, *IEEE Electron Device Lett.*, **EDL-6**, 491 (1985).
3. G.E. Bulman, D.R. Myers, T.E. Zipperian, and L.R. Dawson, *Appl. Phys. Lett.*, **48**, 1015 (1986).

4. J.W. Matthews and A.E. Blakeslee, *J. Crystal Growth*, **27**, 118 (1974).
5. R. Hull, J.C. Bean, F. Cerdeira, A.T. Fiory, and J.M. Gibson, *Appl. Phys. Lett.*, **48**, 56 (1986).
6. H. Asai and K. Oe, *J. Appl. Phys.*, **54**, 2052 (1983).
7. T.E. Van Eck, P. Chu, W.S.C. Chang and H.H. Wieder, *Appl. Phys. Lett.*, **49**, 135 (1986).
8. T.E. Van Eck, P. Chu, W.S.C. Chang and H.H. Wieder, Paper WS1, Optical Society of American Annual Meeting, Seattle, Washington (1986).
9. J.W. Matthews and A.E. Blakeslee, *J. Crystal Growth*, **32**, 265 (1976).
10. D.A.B. Miller, D.S. Chernla, T.C. Damon, A.C. Gossard, W. Wiegmann, T.H. Wood and C.A. Burrus, *Appl. Phys. Lett.*, **45**, 13 (1984).
11. B.F. Aull, W.D. Goodhue, B.E. Burke, and K.B. Nichols (to be published in *Appl. Phys. Lett.*).
12. T.E. Van Eck, L.M. Walpita, W.S.C. Chang and H.H. Wieder, *Appl. Phys. Lett.*, **48**, 451 (1986).
13. D. Psaltis, D. Casasent and M. Carlotto, *Optics Lett.*, **4**, 348 (1979).

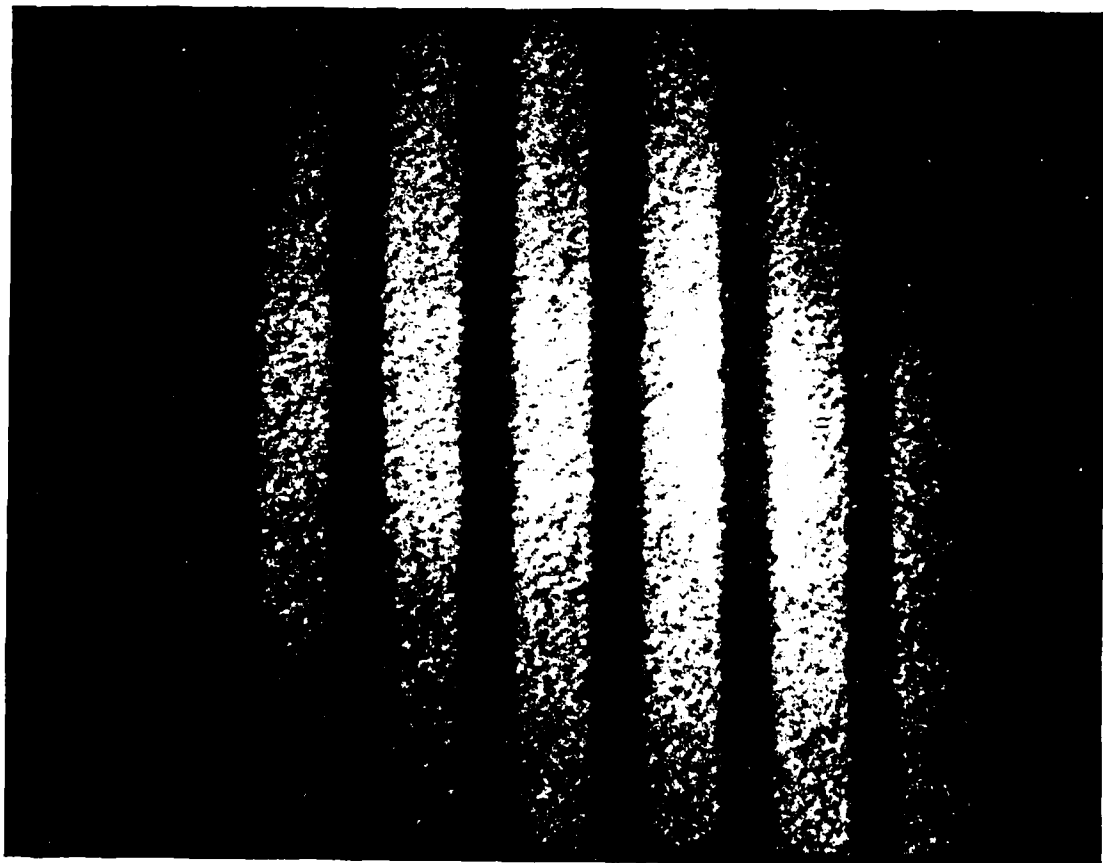


Figure 1. Cross-sectional transmission electron microscope photograph of MBE-110.

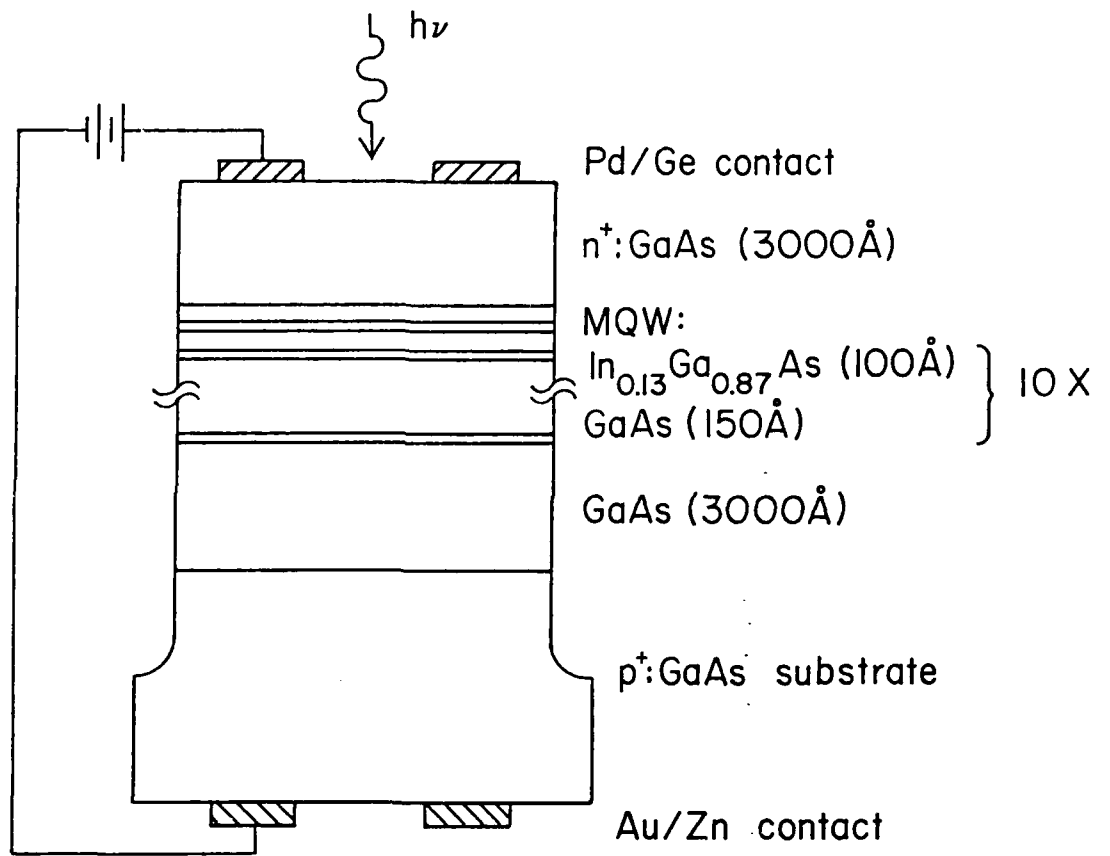


Figure 2. Schematic diagram of sample MBE-110

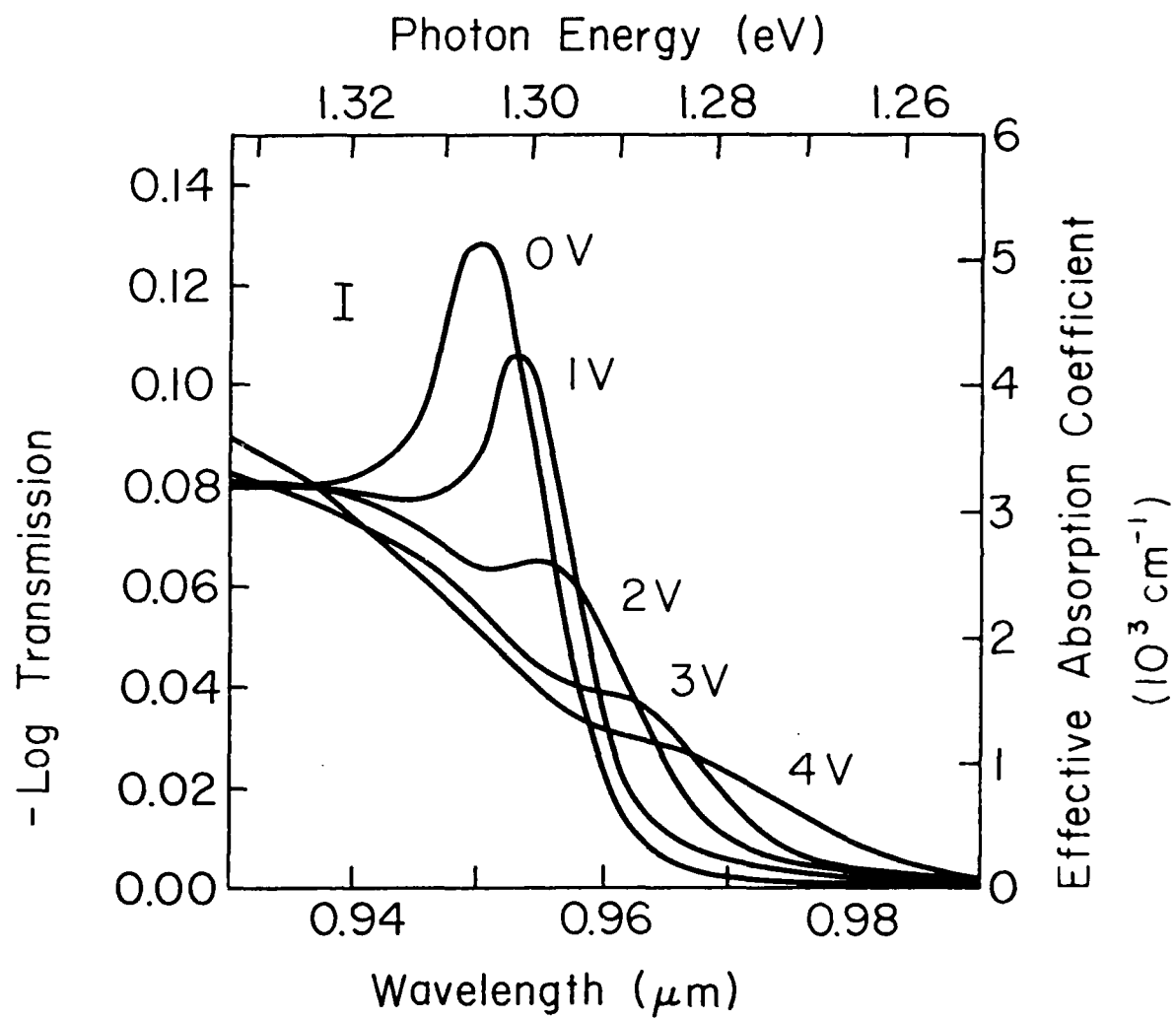


Figure 3. Electroabsorption spectra of sample MBE-110.

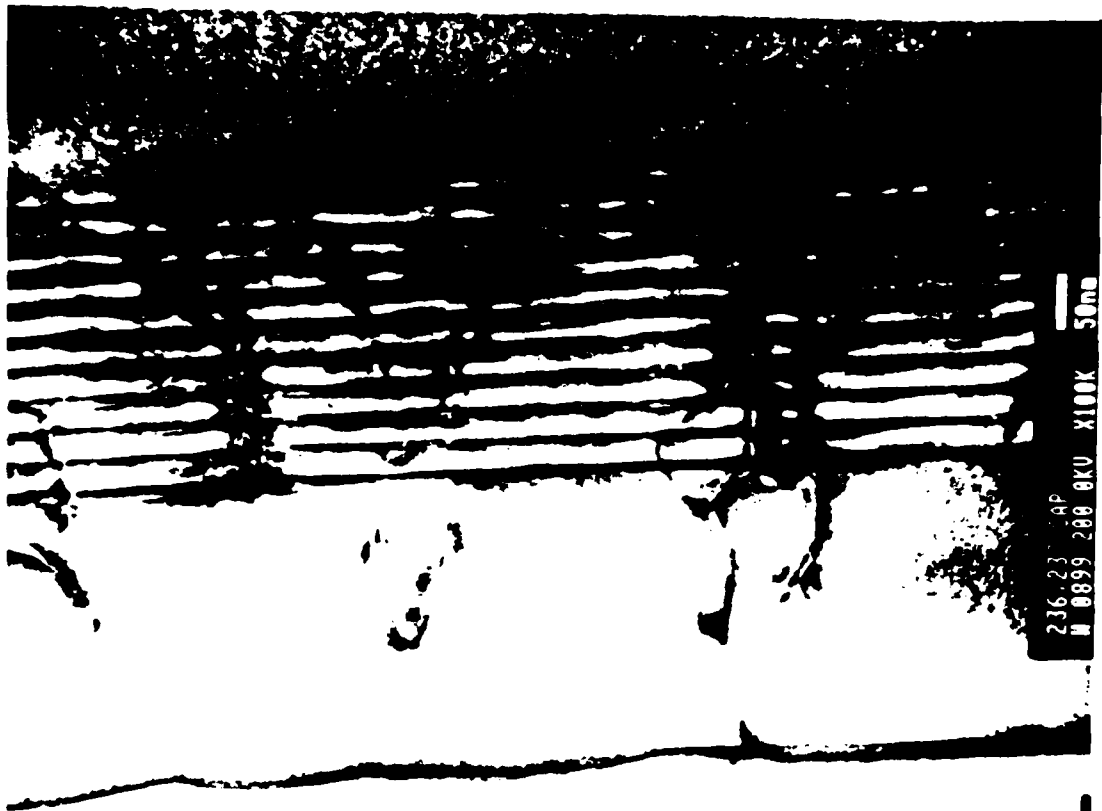


Figure 4. Cross-sectional transmission electron microscope photograph of MBE-236, showing a high density of dislocations.

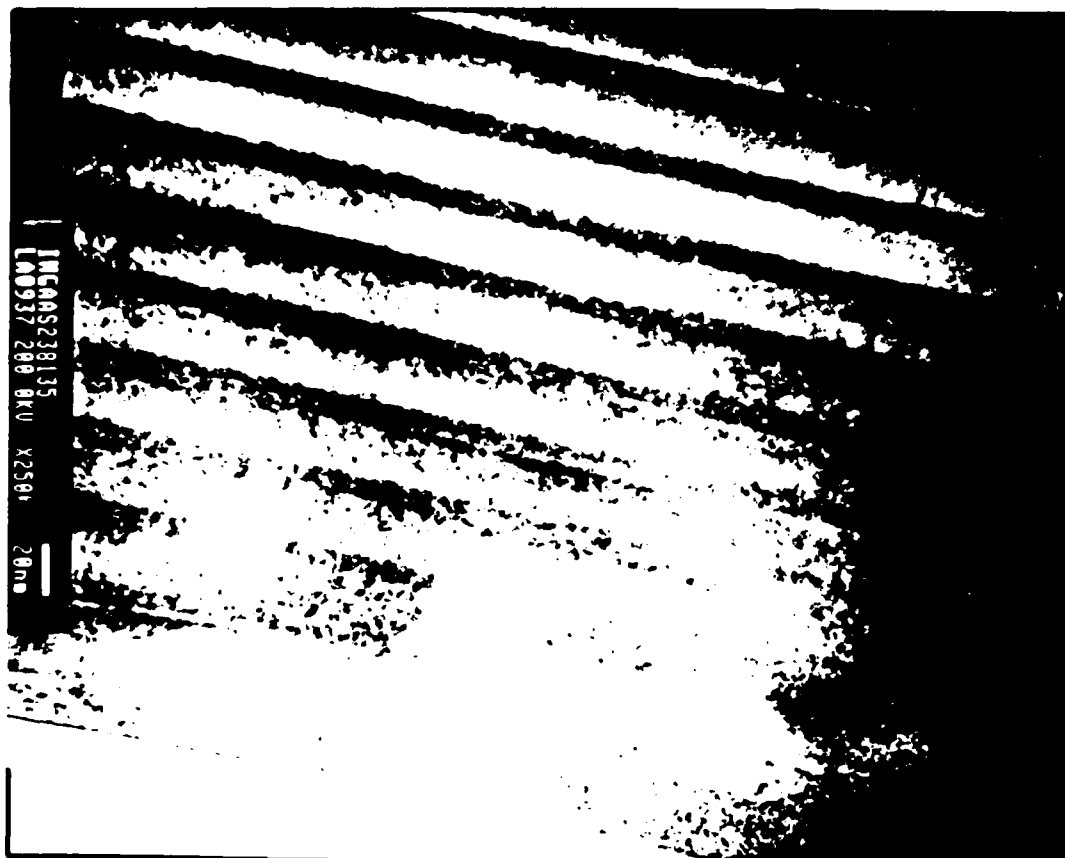


Figure 5. Cross-sectional transmission electron microscope photograph of MBE-238, showing no dislocations.

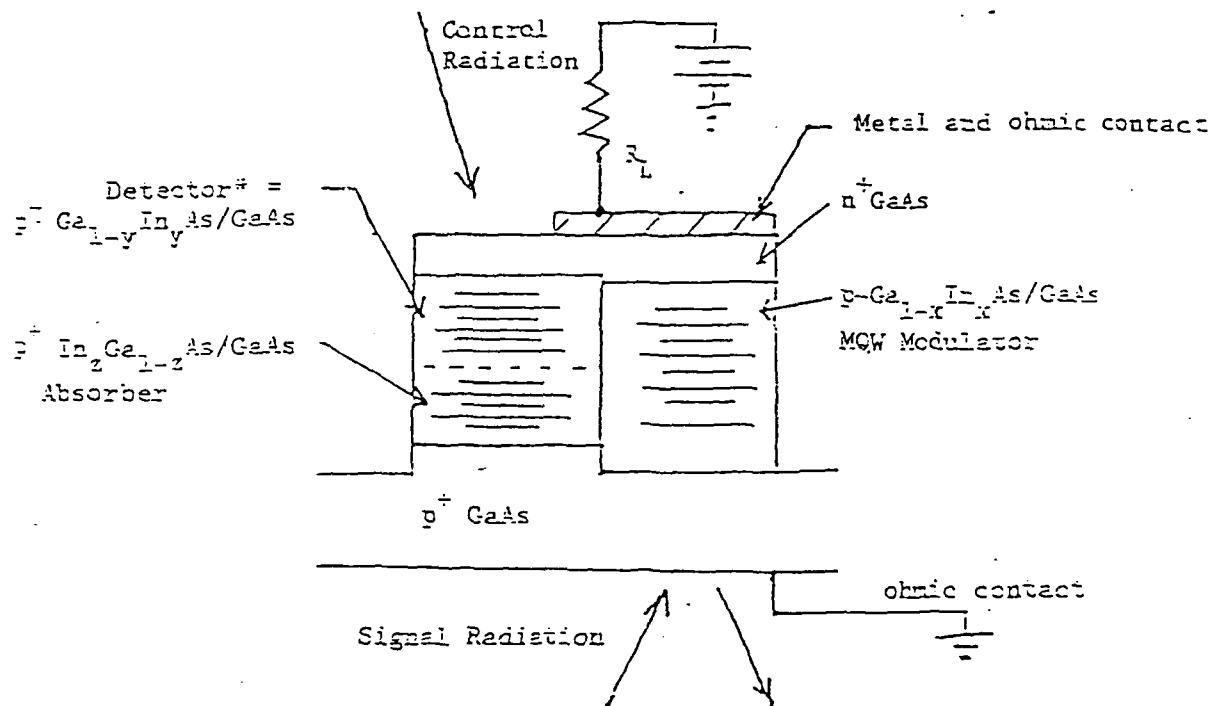


Figure 6. A proposed scheme for a unit cell of a InGaAs/GaAs MQW spatial light modulator.

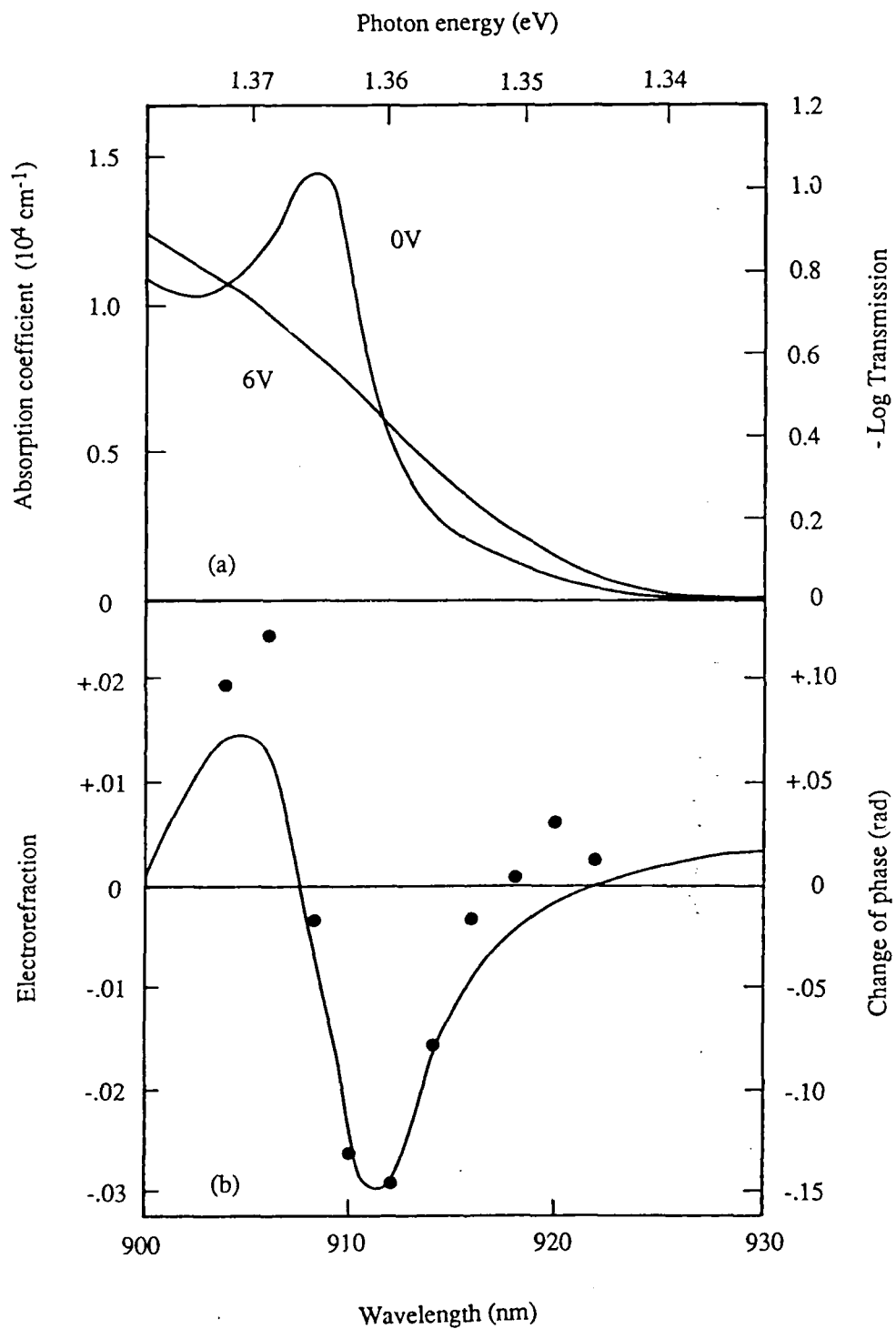


Figure 7. (a) Absorption spectra and (b) electrorefraction spectra of the 60 quantum well InGaAs/GaAs structure fabricated at MIT Lincoln Laboratory.

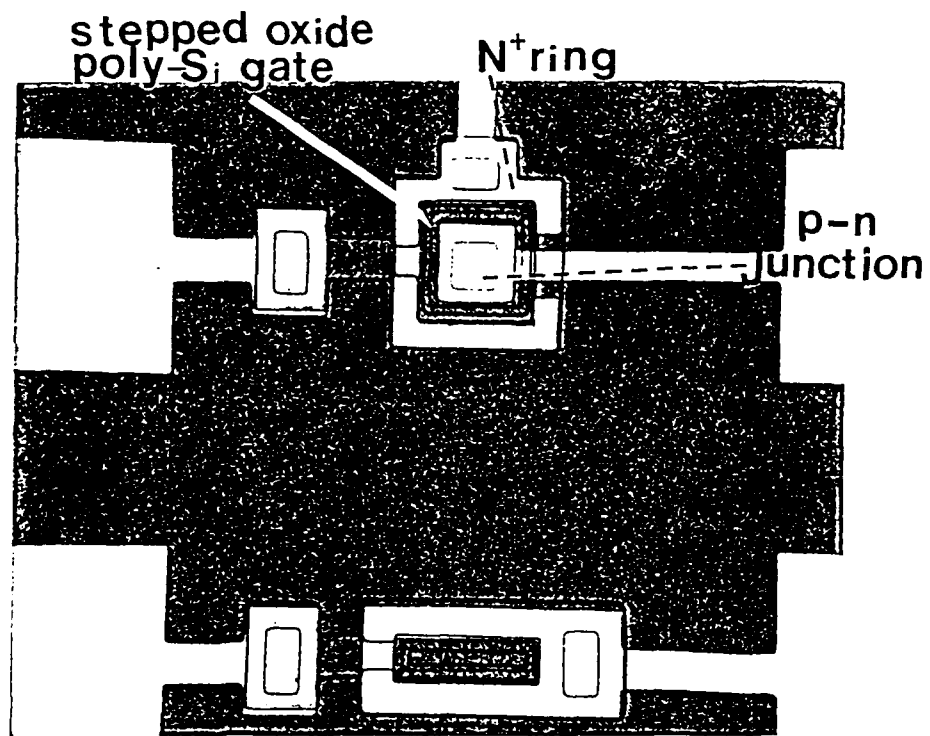


Figure 8. GCPD with stepped gate-oxide

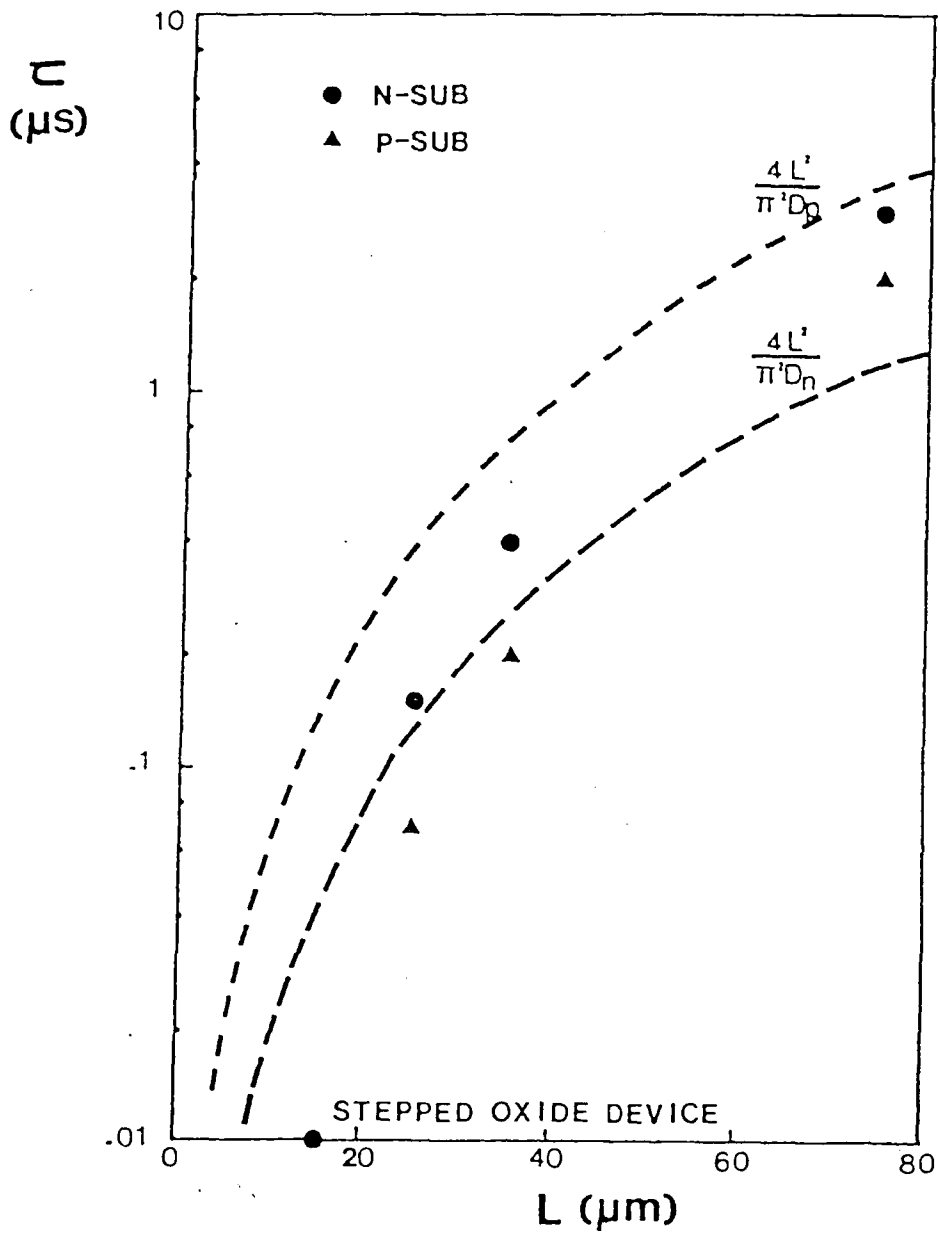


Figure 9.

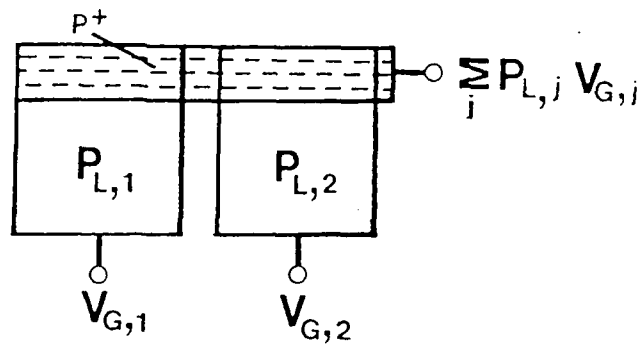
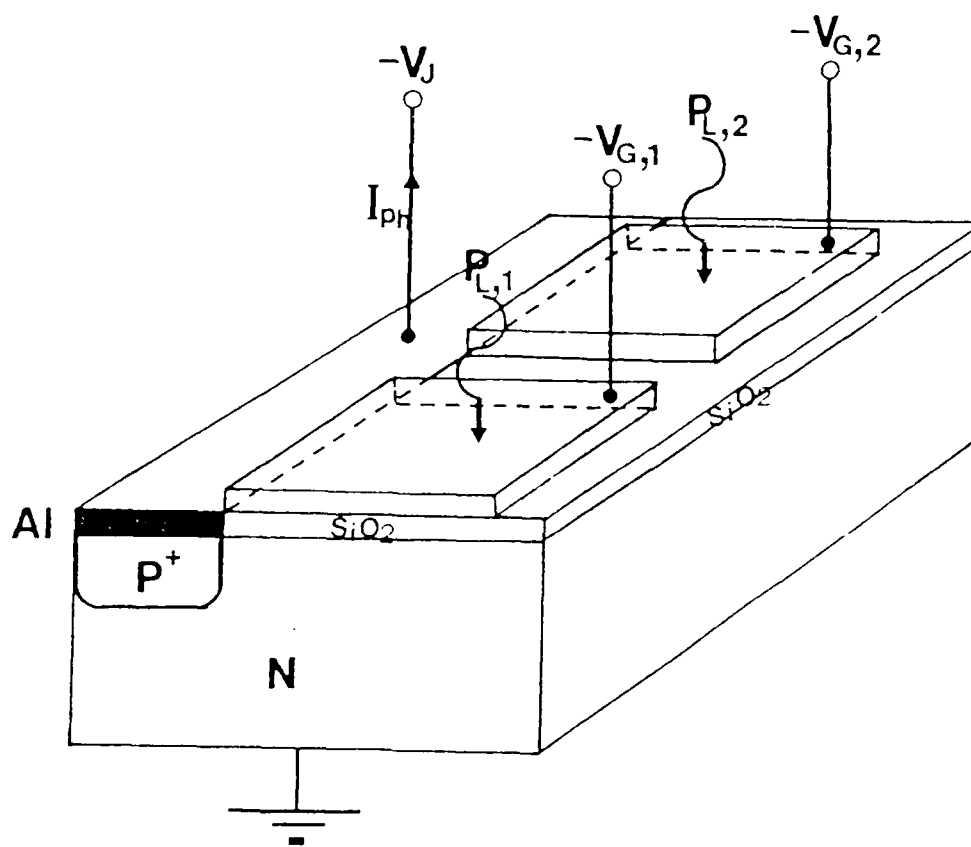
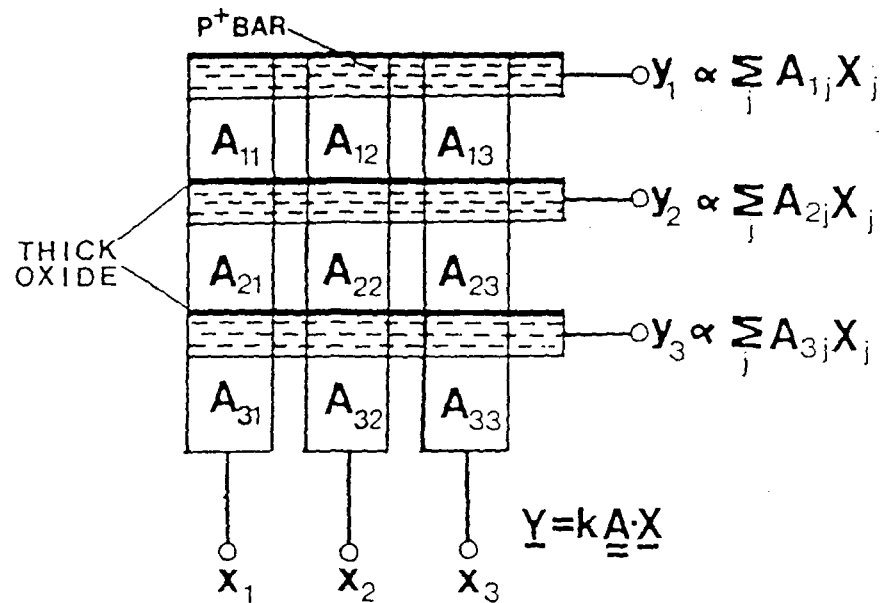


Figure 10. GCPD's connected in parallel.



$$\begin{pmatrix} Y_1 \\ Y_2 \\ Y_3 \end{pmatrix} = K \begin{pmatrix} A_{11} & A_{12} & A_{13} \\ A_{21} & A_{22} & A_{23} \\ A_{31} & A_{32} & A_{33} \end{pmatrix} \begin{pmatrix} X_1 \\ X_2 \\ X_3 \end{pmatrix}$$

$$A_{ij} = P_{L,ij}$$

$$X_j = V_{G,j}$$

Figure 11. Schematic illustration of a GCPD multiplier array.

$$\vec{B} = \vec{A} - \vec{I}$$

$$\underline{X}_{i+1} = \underline{Y} - \vec{B} \underline{X}_i = (\vec{I} - \vec{A}) \underline{X}_i + \underline{Y}$$

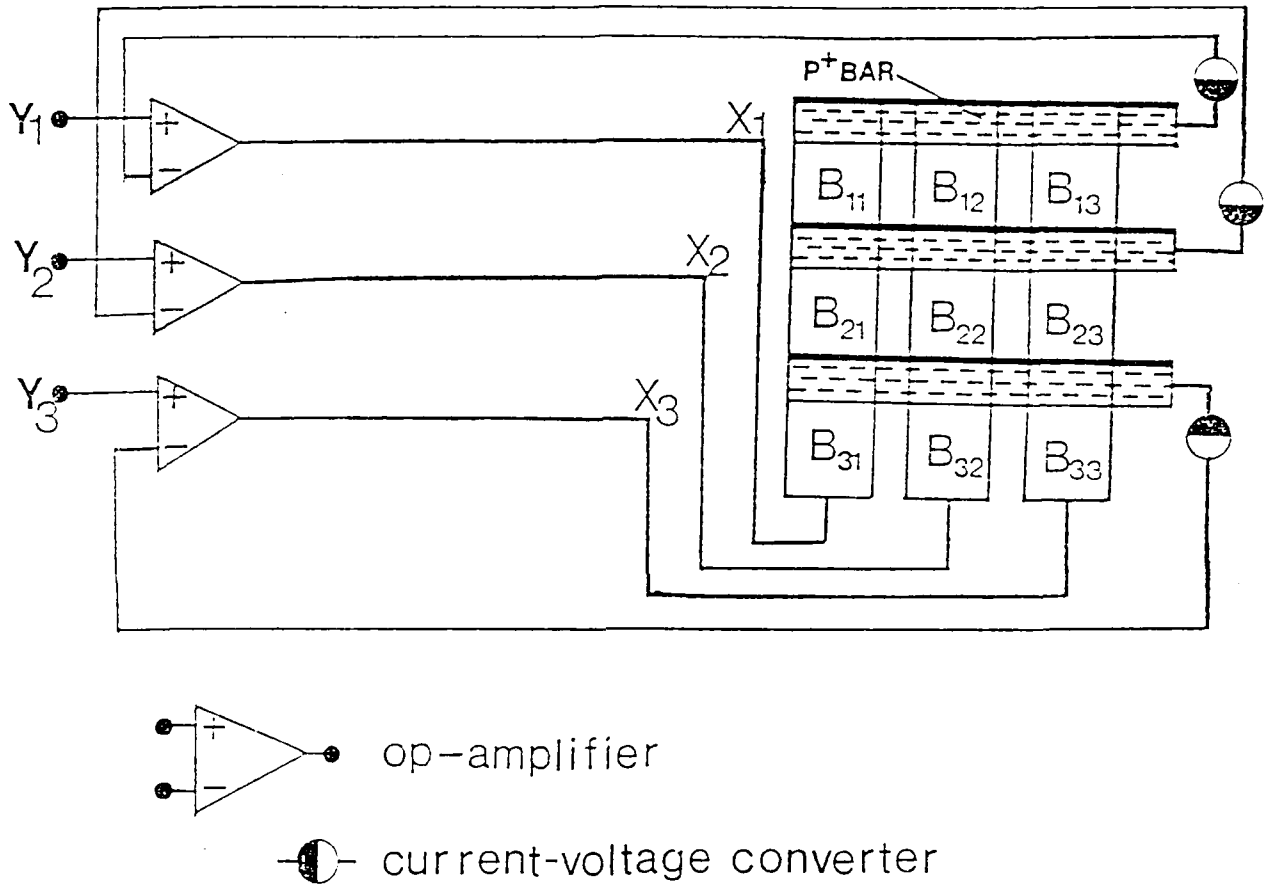


Figure 12. The Optical Matrix Inverter (Relaxation Method.)

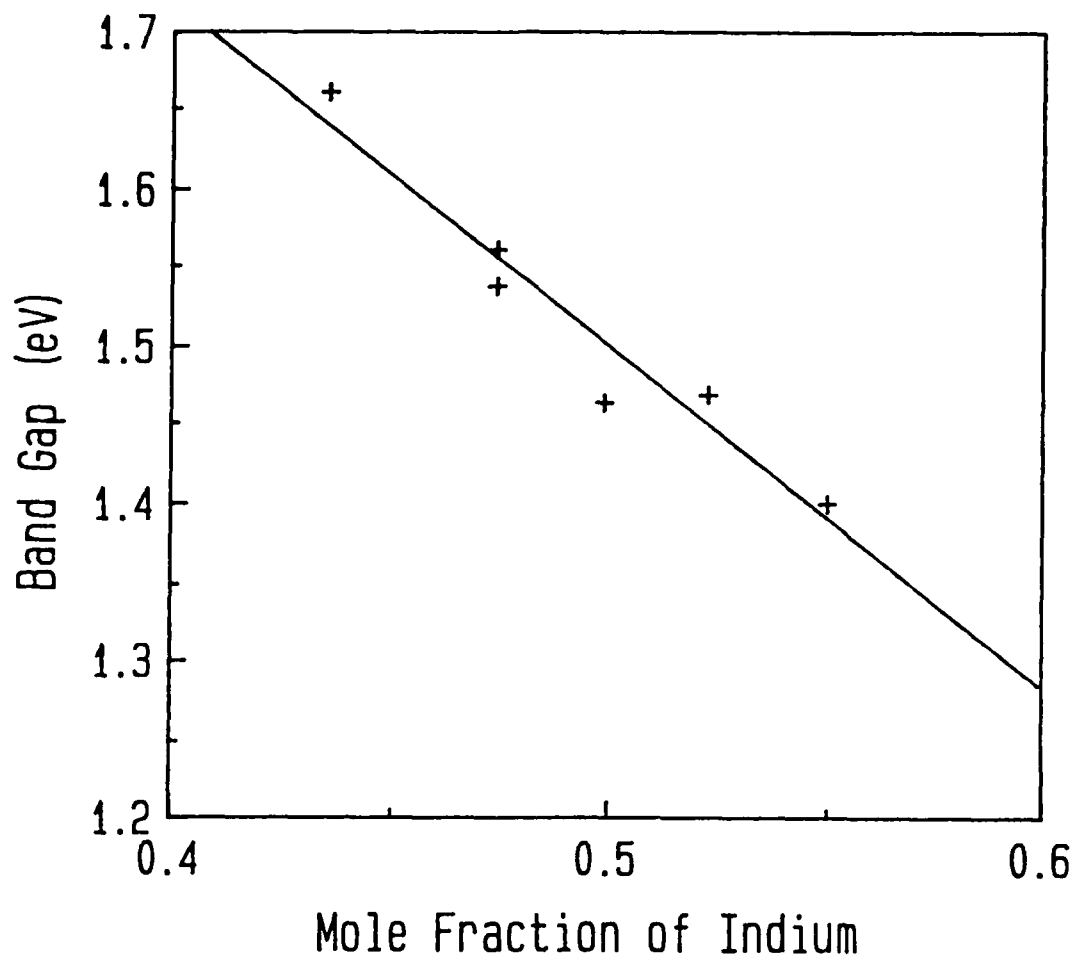


Fig. 13 Room temperature band gap of MBE grown  $\text{In}_x\text{Al}_{1-x}\text{As}$  as a function of the mole fraction  $x$  of indium. The band gap is measured by photoluminescence. The mole fraction of indium is determined by measuring the lattice parameter of the  $\text{In}_x\text{Al}_{1-x}\text{As}$  by double-crystal x-ray diffraction and applying Vegard's law.

END

4-~~2~~-87

DTIC